Corynebacterium matruchotii fitness enhancement of adjacent streptococci by multiple mechanisms

Authors: [1]Eric Almeida*, [2]Surendra Puri*, [2]Subhashini Elangovan, [2]Jiyeon Kim, [1]Matthew Ramsey**

* indicates authors contributed equally

Institutional Affiliations: [1]The University of Rhode Island, Department of Cell and Molecular Biology, [2]The University of Rhode Island, Department of Chemistry, Kingston RI 02881.

** Corresponding author: 120 Flagg Rd. Kingston, RI 02881, 401-874-9505, mramsey@uri.edu

Competing Interests: none

Abstract

Polymicrobial biofilms are present in many environments particularly in the human oral cavity where they can prevent or facilitate the onset of disease. While recent advances have provided a clear picture of both the constituents and their biogeographical arrangement, it is still unclear what mechanisms of interaction occur between individual species in close proximity within these communities. In this study we investigated two mechanisms of interaction between the highly abundant supragingival plaque (SUPP) commensal *Corynebacterium matruchotii* and *Streptococcus mitis* which are directly adjacent *in vivo*. We discovered that *C. matruchotii* enhanced the fitness of streptococci dependent on its ability to detoxify streptococcal-produced hydrogen peroxide and its ability to oxidize lactate also produced by streptococci. We demonstrate that the fitness of adjacent streptococci was linked to that of *C. matruchotii* and that these mechanisms support the previously described “corncob” arrangement between these species but that this is favorable only in aerobic conditions. Further we utilized scanning electrochemical microscopy (SECM) to quantify lactate production and consumption between individual bacterial cells for the 1st time, revealing that lactate oxidation provides a fitness benefit to *S. mitis* and not pH mitigation. This study describes mechanistic interactions between two highly abundant human commensals that can explain their observed *in vivo* spatial arrangements and suggest a way by which they may help preserve a healthy oral bacterial community.

Introduction

Over the past decades our knowledge of the human oral microbiome has increased drastically, revealing a robust polymicrobial biofilm in supragingival plaque (SUPP) that is present in healthy as well as diseased conditions. While we know a great deal about what bacteria reside in SUPP (Benítez-Páez et al., 2014; Eren et al., 2014; Schoilew et al., 2019; Xiao et al., 2016), we know very little about the interactions between taxa especially in healthy conditions relative to disease. Given that dysbiosis of the healthy microbiota is often a prelude to oral disease, we wish to study interactions within the healthy community to potentially reveal any community members that might help preserve stable community structure and constituency, potentially preventing the onset of disease.

Previous studies have shown the importance of attachment to the development of the oral biofilm (Kolenbrander et al., 2006) and new data has identified and refined the spatial organization of abundant commensal organisms found in SUPP (Mark Welch et al., 2016). Human microbiome project (HMP) data and recent microscopy of healthy individuals has revealed that one of the most abundant and prevalent species in SUPP is *Corynebacterium matruchotii* (Mark Welch et al., 2016; Schoilew et al., 2019; Xiao et al., 2016). It has been correlated with good dental health and hypothesized to be important in the organization of some plaque biofilm structures particularly due to its ability to adhere to *Streptococcus* species forming a structure referred to as a “corncob” with the *Corynebacterium* filament being surrounded by streptococci (Mark Welch et al., 2016), a role typically ascribed to *Fusobacterium* (Foster and Kolenbrander, 2004; Kolenbrander et al., 2006). Also, *C. matruchotii* has shown *in vitro* to be able to co-aggregate with *Actinomyces* species which are known to be early colonizers during the plaque biofilm formation (Esberg et al., 2020). It’s been hypothesized that *C. matruchotii* binds to an existing biofilm of *Streptococcus* and *Actinomyces* cells for attachment and anchoring to the plaque (Esberg et al., 2020; Mark Welch et al., 2016). The spatial organization of microbes in SUPP has been characterized in the ‘hedgehog’ model (Mark Welch et al., 2016) which visualizes *C. matruchotii* and its proximity to adjacent *Streptococcus* species, such as *S. mitis* at the SUPP perimeter (Mark Welch et al., 2016; Morillo-lopez et al., 2021).

Streptococcus species, such as *S. mitis*, are one of the most abundant species in the oral microbiome (Eren et al., 2014). *Streptococcus* species have deployed many tactics to compete in their environment such as producing antimicrobial metabolites like H_2O_2 (Redanz et al., 2018) through the activity of pyruvate oxidase (*spxB*) which takes pyruvate, phosphate, and molecular oxygen and converts them into acetyl phosphate, CO_2, and H_2O_2 (Abranches et al., 2018). This production of H_2O_2 has been shown to affect the oral community composition and it is hypothesized in this community *Streptococcus* species metabolize oxygen and sugars to produce H_2O_2 and lactate while attached to *C. matruchotii* (Zhu and Kreth, 2012). Other streptococci are reported to co-aggregate with catalase positive organisms to benefit from catalase activity (Jakubovics et al., 2008) and crossfeeding on *Streptococcus*-produced lactate by commensal microbes which enhances their yield has been previously shown (Ramsey et al., 2011). Others have previously hypothesized that *C. matruchotii* and adjacent streptococci would also utilize these same mechanisms in *in vivo* hedgehog structures (Mark Welch et al., 2016). *C. matruchotii* is in close proximity to many streptococci but not much is known about how it endures these stressors. At low pH streptococci can create an environment suitable for the pathogenic *Streptococcus mutans* to thrive in the community and cause caries (Kim et al., 2020; Takahashi, 2005; Van Houte et al., 1991). If interactions between *C. matruchotii* and *S. mitis* create a more stable and healthy plaque formation without enhancing accumulation of H_2O_2 or creation of low pH environments, this relationship could strengthen the plaque’s pathogen excluding properties known as colonization resistance (Abt and Pamer, 2014). Despite their co-proximity and abundance in these structures,

93 little is known about how these organisms interact (Mark Welch et al., 2016). Previous studies
94 have not likely appreciated the role *C. matruchotii* plays in bridging early and late colonizers within
95 the plaque (Foster and Kolenbrander, 2004; Kolenbrander et al., 2006) and its importance in the
96 structuring of the plaque community. *C. matruchotii*, in close proximity with *S. mitis*, faces the task
97 of detoxifying the streptococcal-produced metabolites being excreted into the environment. This
98 paper focuses on how *C. matruchotii* interact biochemically with H_2O_2 and lactate produced by *S.*
99 *mitis.*
100
101 We employed a reductionist approach to investigate the relationship between these species in *in*
102 *vitro* biofilms. We discovered that *S. mitis* obtained a significant increase in growth yield with *C.*
103 *matruchotii* aerobically and this growth benefit is lost anaerobically where *C. matruchotii* growth
104 is inhibited by *S. mitis*. Likewise, when *C. matruchotii* oxidative stress responses were altered its
105 fitness and the coculture benefit to *S. mitis* yield were reduced. We also observed that *C. matru-*
106 *chotii* upregulated lactate catabolism genes when in close proximity with *S. mitis*. Removal of
107 streptococcal-produced lactate by *C. matruchotii* was a contributor to *S. mitis* growth benefit and
108 surprisingly this effect was pH-independent. We also utilized scanning electrochemical micros-
109 copy to demonstrate that lactate catabolism can deplete local concentrations of this organic acid
110 swiftly in real-time at sub-micron scales, implying that acid removal in coculture can occur in ob-
111 served *in vivo* arrangements between these organisms. These data suggests *C. matruchotii* has
112 the ability to maintain *S. mitis* growth in SUPP by aiding in detoxifying reactive oxygen species
113 (ROS) and removing streptococci-produced lactate which likely helps preserve a robust polymi-
114 crobial biofilm *in vivo*.
115
116

Materials and Methods

Strains and media. Strains and plasmids used in this study are listed in Table S1. *C. matruchotii* (ATCC 14266) and *S. mitis* (ATCC 49456) were grown on Brain Heart Infusion media supplemented with 0.5% yeast extract (BHI-YE) at 37°C in a static incubator with 5% CO_2 or in 5% H_2, 10% CO_2 and 85% N_2 in anaerobic conditions. *E. coli* was grown at 37 °C in standard atmospheric conditions with liquid cultures shaken at 200 RPM. Antibiotics were used at the following concentrations: kanamycin 40 µg/ml for *E. coli* and 10 µg/ml for *C. matruchotii*.

Colony biofilm coculture/ buffered coculture/ catalase coculture. Overnight cultures of *C. matruchotii* and *S. mitis* species were grown in Brain Heart Infusion media supplemented with 0.5% yeast extract (BHI-YE) at 37°C in a static incubator with 5% CO_2 or in 5% H_2, 10% CO_2 and 85% N_2 for anaerobic conditions. Colony biofilm assays were carried out as described previously (Merritt et al., 2005). Briefly, A semi permeable 0.22µm polycarbonate membrane filter (Zheng and Stewart, 2002) was placed on solid BHI-YE media (supplemented with 1.6% agar). Ten µl of each culture were spotted on the membrane filters and monocultures were spot with 10µL of BHI-YE. The cultures incubated for 48hr and the membranes were placed in a microcentrifuge tube with 1mL of BHI-YE. The tubes were vortexed to resuspend into media and serially diluted and track plated (Jett et al., 1997) to count colony forming units per mL (CFU/mL). *S. mitis* was counted by using BHI-YE plates and *C. matruchotii* on BHI-YE plates supplemented with 100 µg/ml fosfomycin. Buffered and pH indicator cocultures were carried out with 50mM MOPS and 18mg/mL of phenol red added to BHI-YE. Catalase cocultures were carried out with 100U/mL of catalase added to BHI-YE.

RNAseq experiment and analysis. Mono and cocultures were prepared similar to the colony biofilm coculture with the exception that culture membranes were incubated for 24hr and moved to fresh media for an additional 4hr. Membranes were then removed from solid agar and immediately placed into RNALater (Ambion) where cells were removed by agitation and pelleted by centrifugation. Cell pellets were stored in Trizol reagent at -80°C. Experiments were carried out in biological duplicates. RNA extraction, library preparation and sequencing were then carried out by the Microbial 'Omics Core facility at the Broad Institute. RNASeq libraries were generated using previously described methods (Shishkin et al., 2015). Sequence data was aligned using Bowtie2 (Langmead and Salzberg, 2012) and read counts per coding sequence were called using HTSeq-Count (Anders et al., 2015). Statistical analysis was carried out via DESeq2 (Love et al., 2014) to determine differentially expressed genes. Scripts of this pipeline can be found at https://github.com/dasithperera-hub/RNASeq-analysis-toolkit. Sequence libraries are available through the NCBI short read archive (SRA) under bioproject number PRJNA832032.

Gene deletions. All *C. matruchotii* gene deletions were carried out with sucrose counterselection using a suicide vector derived from pMRKO (Ramsey et al., 2011), pEAKO2 which contains *sacB* from pK19mobsacB (Schgfer et al., 1994). Approximately 1000 bp up and downstream flanking regions for each gene were used for homologous recombination and fragments were cloned into pEAKO2 via Gibson Assembly (Gibson et al., 2009). *C. matruchotii* cells will be made as previously described (Takayama et al., 2003). Transformations were carried out with 50µL of competent cells and 1µg of DNA electroporated with 0.2cm gap cuvettes at 2.5kV voltage, 400Ω resistance, and 25µF capacitance. After electroporation, 950mL of prewarmed BHI-YE will be added to the cuvette and the mixture will be moved to a 46°C heat block for 6 minutes. After heat shock, transformations will be shaken at 250 RPM at 37°C for 4hr. Transformations were plated on BHI-YE Kan_{10} plates and incubated for 4 days at 37°C. Mutants were verified through PCR.

Limiting glucose coculture. Cultures were prepared like colony biofilm coculture described above except for being inoculated into 2mL of liquid defined medium. Modified RPMI medium (Gibco) was used as a base and supplemented with 8mM glucose. Cocultures were inoculated for 48 hrs and track plated to determine CFU/ mL.

Growth curves. Five milliliter cultures of *C. matruchotii* were grown in BHI-YE for 48hr and back diluted in modified RPMI media supplemented with 40mM lactate at an OD_{600} of 0.025. Cultures were incubated statically at 37°C with 5% CO_2. Optical density readings were taken every 4hr over a 72hr period.

Scanning electrochemical microscopy sample preparation. Bacteria were grown overnight in BHI-YE and then washed by centrifugation in defined medium. The defined medium used was an amended version of Teknova EZ RICH (Teknova, M2105). We prepared the medium as described in the manufacturers instructions with the addition of vitamin solution, lipoic acid, folic acid, riboflavin, NAD+ and nucleotides to final concentrations from that of an oral complete defined medium previously described (Brown and Whiteley, 2007) and glucose at 10 mM. Bacteria were grown to an OD600 of 0.5-0.9 and then diluted to final concentrations of 1.2x107 and 6.0x106 CFU of *C. matruchotii* and *S. mitis* respectively in 200 µL of defined medium. This was then incubated at 37°C with 5% CO_2 for 1 h. 10 µL of this solution was then added to a poly-lysine coated glass slide and incubated at 37°C for 15 minutes after which medium was removed by micropipette to remove planktonic cells and ensure only attached cells remained. An additional 10uL of pre-warmed defined medium was then added to the slide. Samples were then transferred to the SECM instrument for further analysis.

Scanning electrochemical microscopy acquisition. Scanning parameters and nano-probe design are similar to methods described previously (Connell et al., 2014; Kim et al., 2014; Kim et al., 2016; Puri and Kim, 2019). A full description of SECM calibration, sample acquisition and metabolite quantification are provided in the Supplemental Materials.

Results

C. matruchotii enhances the growth of *S. mitis* in aerobic conditions

We performed pairwise coculture experiments aerobically and anaerobically with a colony biofilm model (Merritt et al., 2005) on solid medium to quantify growth yield differences between mono- and cocultures of *S. mitis* with *C. matruchotii* (Fig. 1). Using this reductionist approach, we observed a 954-fold increase in growth yield of *S. mitis* in coculture. Unexpectedly, *C. matruchotii* had no significant difference in growth yield with *S. mitis* (Fig. 1A). While previous studies have hypothesized that *C. matruchotii – Streptococcus* interactions occur in aerobic microenvironments within SUPP (Mark Welch et al., 2016; Morillo-lopez et al., 2021), we also performed the same experiment in anaerobic conditions as a comparison (Fig. 1B). Interestingly, the coculture growth benefit for *S. mitis* was lost while *C. matruchotii* growth yield decreased ~130-fold. To investigate how *C. matruchotii* enhances *S. mitis* growth yield in coculture we performed RNAseq to compare mono- vs coculture transcriptome data.

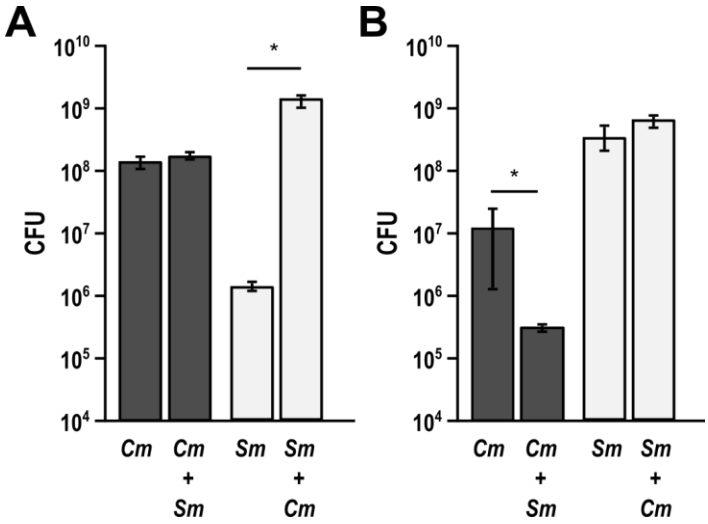

FIG 1 Growth yield measurements of mono vs coculture biofilms. Aerobic (A) and anaerobic (B) CFU counts of *C. matruchotii* (*Cm*) and *S. mitis* (*Sm*) in mono and cocultures. Data are mean CFU counts for n≥3 and error bars represent 1 standard deviation. * denotes $p < 0.05$ using a Student's t-test.

C. matruchotii upregulates genes necessary for L-lactate catabolism and oxidative stress response

C. matruchotii differentially expressed only 22 genes (greater than 2-fold) in aerobic coculture with *S. mitis* (Table S2). Interestingly, C. *matruchotii* upregulated the *lutABC* operon (*lutA,* 4.37-fold; *lutB,* 3.76-fold; *lutC*, 3.20-fold), whose gene products in *Bacillus subtilis* catabolize L-lactate (Chai et al., 2009) using oxygen as a terminal electron acceptor; therefore, in the absence of oxygen, *C. matruchotii* is no longer able to catabolize L-lactate, as previously shown (Iwami et al., 1972). *C. matruchotii* also significantly upregulates a bacterial non-heme ferritin-encoding gene (2.39-fold) in coculture. This protein has been characterized in *Mycobacterium smegmatis* to sequester ferrous ions as part of the oxidative stress response (Smith, 2004). Given the coculture growth and transcriptome results, we broadly hypothesized that *C. matruchotii* crossfeeds on *S.*

mitis-produced lactate while detoxifying *S. mitis*-produced H_2O_2 similar to other microbes in the oral cavity (Jakubovics et al., 2008; Ramsey et al., 2011). Given the fact that *C. matruchotii* cannot utilize L-lactate anaerobically and *S. mitis* is only provided a growth benefit in the presence of oxygen, we believe these data suggest one mechanism by which the biogeography of these species *in vivo* could be influenced by their metabolic interactions.

Lactate utilization by *C. matruchotii* influences *S. mitis* growth yield

The growth enhancement of *S. mitis* in coculture with *C. matruchotii* is likely due to several factors including H_2O_2 decomposition and lactate catabolism. It is unclear if the removal of lactate itself or the removal of lactate and subsequent increase in pH is responsible for *S. mitis* growth yield enhancement. We 1st tested the impact of pH by performing growth experiments in the same medium with increased buffer capacity by adding 50 mM MOPS. Qualitatively, we observed that *S. mitis* monoculture colonies no longer produced yellow coloration in buffered medium containing the pH indicator dye phenol red (i.e. no longer acidified the environment) compared to the original medium (data not shown). Quantitatively, we observed that *S. mitis* growth yield had no significant change in monoculture with additional MOPS (Fig. S1) indicating that pH was likely not responsible for *S. mitis* growth yield increases in coculture.

To determine if removal of lactate by *C. matruchotii* via catabolism was enhancing streptococcal fitness we constructed a *lutA* gene deletion mutant (*ΔlutA*) since each gene within the *lutABC* operon had been described to be essential for L-lactate catabolism (Chai et al., 2009). The *ΔlutA* strain was significantly impaired in L-lactate utilization showing a diminished growth rate (doubling times of 17.9h for the wt and 27.4h for *ΔlutA*) and yield aerobically with L-lactate as the sole carbon source (Fig. S2). A full *lutABC* operon deletion strain was also created and showed similar results (data not shown). In *B. subtilis*, each gene within the *lutABC* operon is essential for lactate oxidation and it can no longer use lactate as its sole carbon source (Chai et al., 2009). *C. matruchotii* possesses two additional annotated L-lactate dehydrogenases which may function bidirectionally allowing it to more slowly oxidize L-lactate without a functional *lutABC* system.

We next tested the *ΔlutABC* mutant in mono vs coculture with *S. mitis* to determine if impaired lactate utilization led to a decrease in *S. mitis* yield in coculture with *C. matruchotii*. Using defined medium in glucose-limited conditions to force the bacteria to compete for the limited carbon source and/or promote cross-feeding on streptococcal produced lactate, we performed mono vs cocultures and determined that both *S. mitis* and *C. matruchotii* Δ*lutABC* fitness were significantly decreased in coculture (Fig. 2). *C. matruchotii ΔlutABC* can only poorly catabolize L-lactate and thus poorly cross-feed on *S. mitis*-produced L-lactate compared to the wildtype. As *ΔlutABC* and *S. mitis* are now forced to compete for limited glucose, both exhibit a decreased growth yield. This is in agreement with previous data anaerobically (Fig. 1B), where lactate oxidation by *C. matruchotii* does not occur. The growth yield increase of *S. mitis* in coculture is diminished when *C. matruchotii* cannot oxidize lactate but this does not fully explain the total growth benefit provided, suggesting another mechanism(s) at work.

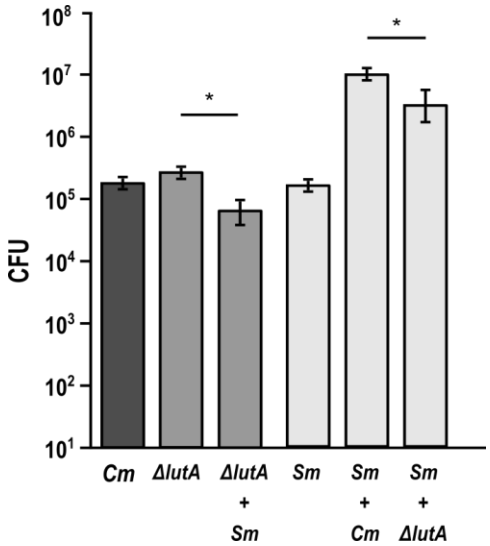

FIG 2 Limiting glucose colony biofilm cocultures. CFU counts of *C. matruchotii* (*Cm*), *C. matruchotii ΔlutA*, and *S. mitis* (*Sm*) in mono and cocultures. Data are mean CFU counts for n≥3 and error bars represent 1 standard deviation. * denotes p< 0.05 using a Student's t-test.

Catalase abundance leads to enhanced streptococcal growth yields

Given that lactate oxidation by *C. matruchotii* provides only a small portion of the fitness benefit in coculture to *S. mitis* we next investigated if H_2O_2 detoxification by *C. matruchotii* also contributes to fitness. Surprisingly, in coculture with *S. mitis*, *C. matruchotii* did not upregulate expression of the single catalase (*katA*) encoded on its chromosome. We observed that catalase was already maximally expressed aerobically and not expressed anaerobically (data not shown). To test if catalase-dependent H_2O_2 detoxification was important both for *C. matruchotii* fitness in coculture and subsequent *S. mitis* growth yield enhancement, we generated the catalase gene deletion mutant, *C. matruchotii ΔkatA*. Interestingly, this mutant had to be generated entirely under anaerobic conditions and does not survive incubation in aerobic or microaerophilic conditions (data not shown), making it impossible to test this mutant in aerobic coculture with *S. mitis*. Instead, we determined the contribution of catalase to the growth of these species by adding it exogenously. We performed aerobic mono vs cocultures in growth medium amended with 100U/mL of bovine catalase.

Previous studies (Eisenberg, 1973; Jakubovics et al., 2008; Regev-Yochay et al., 2007) have indicated that streptococcal-produced H_2O_2 is capable of limiting their own growth. We observed that adding exogenous catalase elevated the monoculture growth yield of *S. mitis* 6.42-fold (Fig. 3A). This self-limitation by H_2O_2 production is also observed when comparing monoculture fold changes of *S. mitis* to the non H_2O_2–producing *ΔspxB* mutant (Fig. 3). Interestingly, the growth benefit of *S. mitis* in coculture with *C. matruchotii* dropped from 954-fold to 148-fold when amended with catalase.

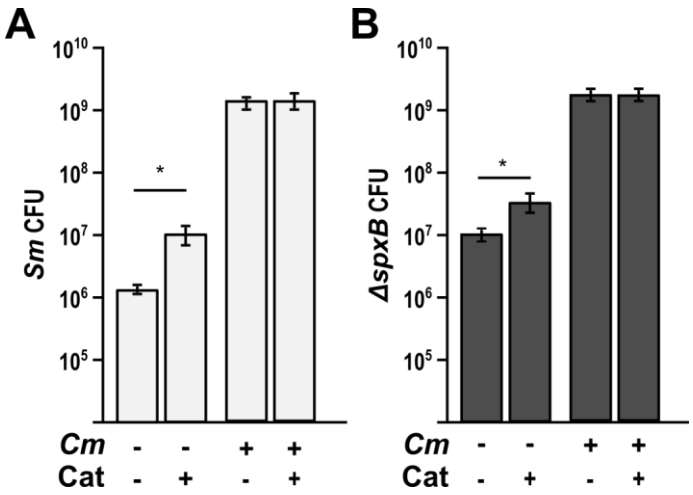

FIG 3 *S. mitis* monoculture enhanced by exogenous catalase. A) CFU counts of *S. mitis* WT (*Sm*) in mono and coculture with *C. matruchotii* (*Cm*) on media containing 100U/mL of catalase vs without. B) CFU counts of *S. mitis ΔspxB* in mono and coculture with *Cm* on media containing 100U/mL of catalase vs without. * denotes $p < 0.05$ using a Student's t-test.

C. matruchotii requires a functional oxidative stress response to be fit to interact with *S. mitis*

In coculture with *S. mitis, C matruchotii* significantly upregulated a gene encoding ferritin, a bacterial non-heme protein involved in oxidative stress response (Smith, 2004). We hypothesized that ferritin was needed for *C. matruchotii* fitness with H_2O_2-producing streptococci. To test this, we deleted the ferritin encoding gene generating *C. matruchotii Δftn* and performed cocultures with WT *S. mitis* and *S. mitis ΔspxB* (which is unable to produce H_2O_2) (Redanz et al., 2018). In coculture with WT *S. mitis*, we observed that the *Δftn* mutant fitness decreased 7.35-fold (Fig. 4A) and this decrease was not observed in coculture with the *S. mitis ΔspxB* strain. *S. mitis* WT had a 4.6-fold significant decrease in growth yield with *C. matruchotii Δftn* compared to *C. matruchotii* WT whereas there was no change in growth yield with *S. mitis ΔspxB* with either *C. matruchotii* strain. This shows that *C. matruchotii* needs a functional oxidative stress response in order to be fit with its interactions with *S. mitis* WT. These data indicate that H_2O_2 detoxification is the largest contributor to enhanced *S. mitis* fitness in coculture but also that other mechanisms, likely *C. matruchotii* lactate oxidation, further enhance fitness.

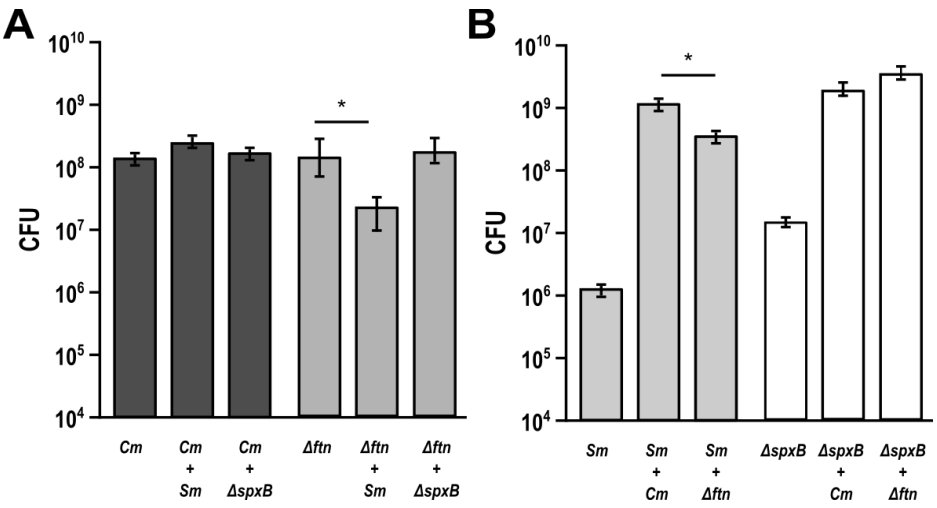

FIG 4 *C. matruchotii* ferritin knockout inhibited when cocultured with *S. mitis*. A) Aerobic CFU counts of *C. matruchotii* WT (*Cm*) and ferritin knockout (*Δftn*) in mono and coculture with *S. mitis* WT and strain lacking ability to create H_2O_2 (*ΔspxB*). B) CFU counts of *Sm* and *ΔspxB* in mono and coculture with *Cm* and *Δftn*. Data are mean CFU counts with error bars indicating standard deviation for n≥3. * denotes p< 0.05 using a Student's t-test compared to monoculture.

Scanning electrochemical microscopy (SECM) reveals oxidation of *S. mitis*-produced lactate by adjacent *C. matruchotii* at sub-micron scale

To investigate lactate production and consumption *in situ* by bacteria as well as the topography of bacterial cells, a submicropipet-supported interface between two immiscible electrolyte solutions (ITIES) was employed (Figs 5, S3) (Puri and Kim, 2019). With this submicrotip, an etched Ni/Cu electrode in the internal organic electrolyte exerts a bias across the submicroscale liquid/liquid interface against an electrode in the aqueous solution (Fig. S3A) to yield the amperometric tip current based on the selective interfacial transfer of a small probe ion (Puri and Kim, 2019). The coculture of *C. matruchotii* and *S. mitis* was immobilized over a poly L-lysine coated glass plate, and studied by scanning or approaching an 800 nm-diameter pipet tip over the bacteria (Fig. S3C). Further detail is provided in the supplemental materials.

We employed the constant-height mode of submicroscale SECM to successfully image single bacterial cells in coculture (Fig. 5). The high spatial resolution was obtained by using submicropipet tips, which were characterized by cyclic voltammetry for tetraethylammonium (TEA+) ion transfer (IT) in situ to obtain a diffusion limited current in the bulk solution, $i_{T,\infty}$ (120 pA). The submicrotip approached the glass substrate until the tip current decreased to 90 % of $i_{T,\infty}$, which is equivalent to the tip-substrate distance, *d*, of 0.85 µm with the tip radius, *a*, of 430 nm. Further, a tip was withdrawn 1.75~2.00 µm higher, and scanned laterally at the fixed height while the tip current was monitored to obtain an SECM image (Fig. S3D). Constant-height imaging of cocultured bacteria for the probe ion TEA was obtained with the gap between the tip and bacteria, d_c = 0.75 µm, i.e., 1.80 normalized distance to tip radius, (*d/a*). This SECM image could not resolve each individual bacterial cell. For instance, a lump was identified in 25 µm × 20 µm image based on TEA^+ IT, which did not resolve any difference between bacterial cells (Fig. 5B). Low tip currents of ~ 80 % of $i_{T,\infty}$ for TEA^+ above these bacteria was obtained due to hindered diffusion of TEA^+ by

adjacent bacteria with membranes near impermeable to this probe ion. As shown in the chronoamperometric responses (shown as raw data in Fig. 5D, cross sections of the SECM image in Fig. 5B), currents were monotonically lowered in 1450~1650 s (positive polarity for cationic currents).

The same area in 25 μm × 20 μm was imaged based on lactate IT with the gap between the tip and bacteria, d_c = 0.50 μm (1.20 *d/a*), which could resolve individual *S. mitis* and *C. matruchotii* clearly (Fig. 5C). An initial current, ~30 pA above a glass substrate corresponds to 0.26 mM of lactate produced by ensemble of bacteria and diffused to bulk solution near bacteria according to eq 1 below.

$$i_{T,\infty} = 4xzFDCa \qquad \text{(eq 1)}$$

where $i_{T,\infty}$ is a current in bulk, *x* is the function of RG ratio (RG is the ratio of outer and inner diameters of a glass pipet, 1.16 for a RG 1.5 tip), *z* is charge of lactate, *F* is Faraday constant (96485 C/mol), *D* is the diffusion coefficient (6×10^{-6} cm^2/s), *C* is a concentration of lactate (0.26 mM), and *a* is the inner radius of a pipet tip (430 nm).

In this SECM image, high tip currents, 50 pA of 166 % of $i_{T,\infty}$ for lactate are obtained above spherical *S. mitis*, while low tip currents, 22 ~24 pA of 75~80 % of $i_{T,\infty}$ are observed above filamentous *C. matruchotii*. Not only distinctive morphologies are clearly distinguished between two different bacteria as shown in optical microscopic image (Fig. 5A), but also the production and consumption of lactate between them are visually confirmed *in situ*. As shown in chronoamperometric responses (shown as raw data in Fig. 5E, cross sections of the SECM image in Fig. 5C), currents were dramatically transposed from an enhanced response over *S. mitis* to reduced ones over *C. matruchotii* (negative polarity for anionic currents), implying local increase in lactate produced by *S. mitis* and local depletion of lactate consumed by *C. matruchotii*. Notably, this SECM image successfully visualized the chemical interaction between two commensal oral microbes in real time and is the 1st SECM study to our knowledge that measures metabolite exchange between two individual bacterial cells. Specifically, *S. mitis* produces ~0.52 mM lactate locally, which is efficiently depleted by C. *matruchotii* (Figs. 5, S4) thus verifying a standing question about their commensal relationship that cannot be answered only by optical microscopic imaging. Quantitative analysis of the permeability of the bacterial membrane and the local concentration of lactate produced by *S. mitis* are discussed in the supplemental materials.

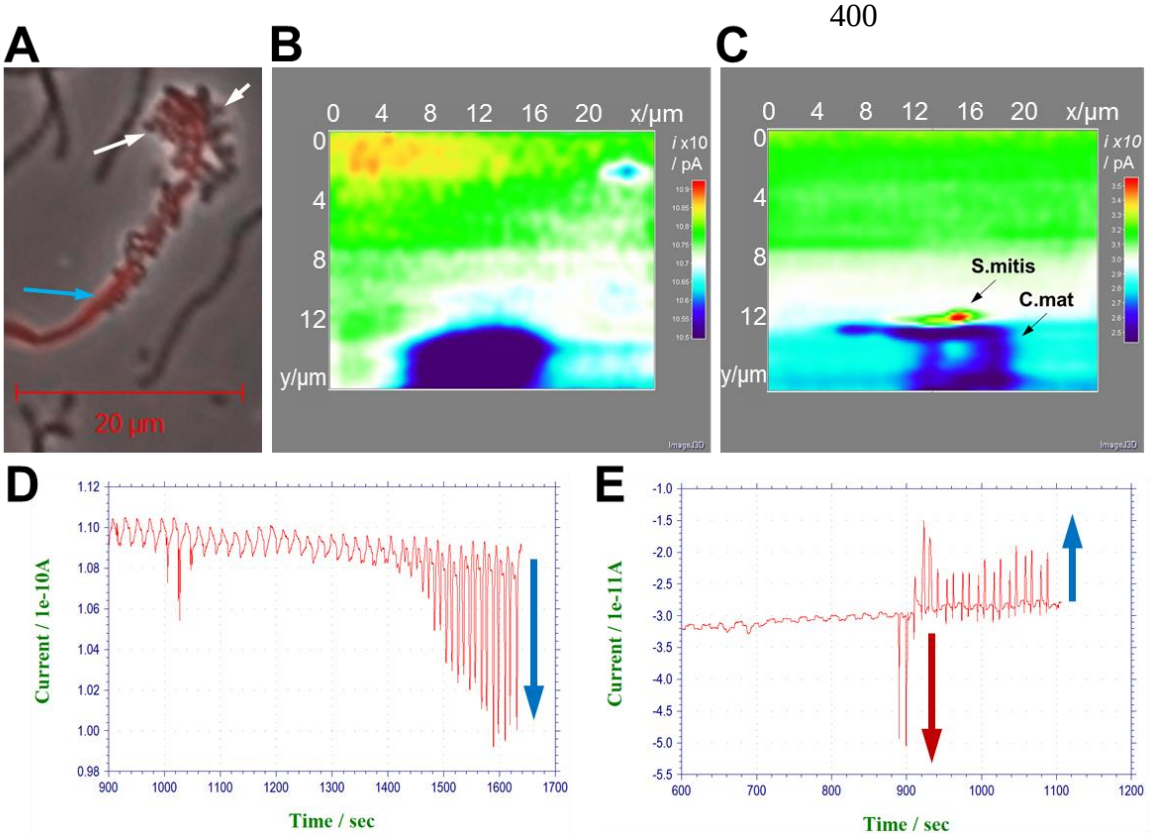

FIG 5 (A) Optical microscopic image of *C. matruchotii* (blue arrow) and *S. mitis* (white arrows) coculture. Constant-height SECM images based on (B) TEA^+ IT (obtained with a gap between the tip and bacteria, d_c = 1.8 *d/a*) and (C) lactate IT (obtained at d_c = 1.2 *d/a*) , Chronoamperometric responses based on (D) TEA^+ IT and (E) lactate IT (raw data, cross sections of SECM images in (B) and (C), respectively). The current polarity is set to positive for cationic current response and negative for anionic current response.

Discussion

Interactions between commensal bacteria within healthy SUPP are understudied for their role in maintaining plaque homeostasis and host health compared to subgingival plaque and oral disease (Foster and Kolenbrander, 2004; Guggenheim et al., 2001; Kolenbrander et al., 2006). While the organisms in SUPP are in close proximity to one another and capable of physical and biochemical interaction, these mechanisms are largely hypothetical (Mark Welch et al., 2016). Characterizing the behavior of abundant SUPP commensal organisms can help reveal necessary interactions that could maintain a healthy microbiome. One set of interactions are those between *Corynebacterium matruchotii*, and *Streptococcus* spp in previously described 'hedgehog' structures (Mark Welch et al., 2016; Morillo-lopez et al., 2021) where they occur at the presumed aerobic biofilm / saliva margin. This study investigates these interactions and provides novel data on metabolite exchange between individual cells that has broad implications on polymicrobial biofilms beyond the human oral cavity.

Our data indicates that *S. mitis* had a significant growth yield increase when cocultured with *C. matruchotii* (Fig. 1A) and this growth benefit was lost anaerobically (Fig. 1B) which aligns with their proximal association only at the aerobic margin of their biofilm structures (Mark Welch et al., 2016; Morillo-lopez et al., 2021). H_2O_2-producing *Streptococcus* and adjacent commensal species have been shown to coexist despite ROS production (Jakubovics et al., 2008). *C. matruchotii* is uninhibited when cocultured with *S. mitis* aerobically likely due to catalase production. A *C. matruchotii ΔkatA* was created to test this hypothesis and unexpectedly would only grow anaerobically. To confront this limitation and understand the role catalase has on *S. mitis* growth benefit, we added exogenous catalase into the medium to observe if there was a less prominent or loss of growth benefit between mono and coculture *S. mitis* since both now benefit from detoxified ROS. *S. mitis* monocultures on media containing catalase showed increased growth yield (Fig. 3A), confirming the role of catalase in enhancing *S. mitis* fitness. However, even with exogenous catalase there was still a significant increase in *S. mitis* yield in coculture suggesting that *C. matruchotii* provides further growth benefits beyond ROS detoxification.

The fitness of *C. matruchotii* in *S. mitis*-induced oxidative stress is influenced by its ability to not only detoxify H_2O_2 but prevent its reaction with free ferrous ions. This was evident by the expression of a ferritin-like protein in coculture with *S. mitis* that has an 82% protein identity with the ferritin encoded in *Corynebacterium mustelae.* Bacterial ferritin-like proteins have been shown to sequester away iron to avoid the oxidation of ferrous iron to ferric iron (Smith, 2004). Ferritin-like proteins can also bind to DNA for protection from these free hydroxyl radicals (Smith, 2004). Their activity can prevent the production of hydroxyl radicals known to damage DNA and lipids (Winterbourn, 1995). *C. matruchotii Δftn* showed a significant yield decrease in coculture with *S. mitis* but this inhibition was not observed with *S. mitis ΔspxB*. We observed that any decreases in *C. matruchotii* yield were mirrored by decreases in *S. mitis* yield as well, linking streptococcal fitness to that of *C. matruchotii*. We hypothesize that this should also be true for any other adjacent H_2O_2-producing streptococcal species. Transcriptional responses of *S. mitis* to *C. matruchotii* are part of a separate ongoing study and are not reflected here.

C. matruchotii has been shown to only oxidize lactate aerobically and cannot grow on lactate as a sole carbon source anaerobically (Iwami et al., 1972). Of the 22 genes that *C. matruchotii* differentially expresses with *S. mitis* aerobically, three belong to the *lutABC* operon which encodes lactate catabolism genes (Chai et al., 2009). We generated a deletion of the *lut* operon in *C. matruchotii* and found that it could only modestly oxidize lactate (Fig. S2) presumably due to reversible reaction(s) by any/all of 3 other L-lactate dehydrogenases that it encodes. We originally hypothesized that removal of lactate would benefit *S. mitis* by neutralizing the local pH. We tested

this by addition of copious amounts of MOPS buffer but observed no significant changes in growth yield vs medium lacking MOPS. Using the pH indicator phenol red, we were unable to observe acidification around cocultured cells in the presence of additional buffer. Unexpectedly, these data suggest that pH modulation is not a factor in coculture growth yield benefit.

Alternatively, *C. matruchotii* may aid *S. mitis* by the removal of lactate itself and in doing so allow for more glucose fermentation by preventing feedback inhibition. This is further supported by total loss of coculture enhancement of *S. mitis* growth yield observed anaerobically (Fig. 1B). Lactate removal was linked to increased *S. mitis* growth in our limited glucose experiment which forced *C. matruchotii* to rely on lactate produced by *S. mitis* for full growth yield. We saw a significant decrease of *C. matruchotii ΔlutABC* when in coculture with *S. mitis* on limiting glucose media when compared to monoculture and a similar decrease in *S. mitis* yield (Fig. 2). This shows that *C. matruchotii* cannot compete for glucose when in competition with *S. mitis* and likely depends on cross-feeding of lactate when they are in direct proximity.

Using SECM we were able to directly quantify lactate production by *S. mitis* and its oxidation by adjacent *C. matruchotii* in real time (Fig. 5) indicating a sharp decrease in lactate concentration between individual cells. To the best of our knowledge this is the first observation of metabolite exchange between individual bacterial cells by SECM. We believe that existing 'corncob' configurations observed *in vivo* (Mark Welch et al., 2016; Morillo-lopez et al., 2021) should easily be able to consistently remove lactate from their immediate area. This would allow streptococcal metabolism to continue without inhibition while eliminating a source of acid stress to the host and other adjacent microbiota. This observation supports a mechanism whereby the interaction between these two commensals may contribute to the lack of cariogenic activity in a healthy oral biofilm.

This study has described two mechanisms of interaction between bacteria that exist in direct contact *in vivo*. Using a reductionist approach, we were able to ascertain how each mechanism contributed to fitness of both organisms. Advantages provided to each species when these mechanisms are intact also reflect the positional arrangement of these species *in vivo* as anaerobic conditions would not allow for favorable interactions to occur. Additionally, we were able to demonstrate real-time metabolite exchange between these species at sub-micron distances, indicating that crossfeeding between these organisms is likely occurring between them *in vivo*. These interactions reveal one way by which structural orientation and species composition between commensals may contribute to host health and potentially be one way by which a healthy biofilm composition is maintained *in vivo*.

Acknowledgments:
We thank Janet Atoyan and the RI-EPSCOR sequencing facility at URI for sequence generation, Jonathan Livny and the Microbial 'Omics Core and Genomics Platform for their help with RNASeq library sequencing and guidance on experimental design, other members of the Ramsey lab and the Annual Mark Wilson conference attendees for many valuable suggestions and discussion.

Funding Sources: This work was funded by the NIDCR/NIH (R01DE027958 – MR), NIGMS/RI-INBRE early career development award (P20GM103430 - MR), and the USDA National Institute of Food and Agriculture, Hatch Formula project accession number 1017848 (MR).

Author Contributions: MR and JK designed research; EA, SP, and SE performed research, EA, SP, JK and MR wrote the paper.

Competing Interests: The authors declare that there are no competing financial interests with this work.

References

Abranches, J., Zeng, L., Kajfasz, J.K., Palmer, S.R., Chakraborty, B., Wen, Z.T., Richards, V.P., Brady, L.J., Lemos, J.A., 2018. Biology of Oral Streptococci. Microbiology Spectrum 6, 1–18. https://doi.org/10.1128/microbiolspec.gpp3-0042-2018

Abt, M.C., Pamer, E.G., 2014. Commensal bacteria mediated defenses against pathogens. Current Opinion in Immunology 29, 16–22. https://doi.org/10.1016/j.coi.2014.03.003

Anders, S., Pyl, P.T., Huber, W., 2015. HTSeq-A Python framework to work with high-throughput sequencing data. Bioinformatics 31, 166–169. https://doi.org/10.1093/bioinformatics/btu638

Benítez-Páez, A., Belda-Ferre, P., Simón-Soro, A., Mira, A., 2014. Microbiota diversity and gene expression dynamics in human oral biofilms. BMC Genomics 15, 1–13. https://doi.org/10.1186/1471-2164-15-311

Brown, S.A., Whiteley, M., 2007. A Novel Exclusion Mechanism for Carbon Resource Partitioning in *Aggregatibacter actinomycetemcomitans*. J Bacteriol 189, 6407–6414. https://doi.org/10.1128/JB.00554-07

Chai, Y., Kolter, R., Losick, R., 2009. A widely conserved gene cluster required for lactate utilization in Bacillus subtilis and its involvement in biofilm formation. Journal of Bacteriology 191, 2423–2430. https://doi.org/10.1128/JB.01464-08

Connell, J.L., Kim, J., Shear, J.B., Bard, A.J., Whiteley, M., 2014. Real-time monitoring of quorum sensing in 3D-printed bacterial aggregates using scanning electrochemical microscopy. Proc. Natl. Acad. Sci. U.S.A. 111, 18255–18260. https://doi.org/10.1073/pnas.1421211111

Eisenberg, R.J., 1973. Induction of unbalanced growth and death of Streptococcus sanguis by oxygen. Journal of Bacteriology 116, 183–191. https://doi.org/10.1128/jb.116.1.183-191.1973

Eren, a M., Borisy, G.G., Huse, S.M., Mark Welch, J.L., 2014. Oligotyping analysis of the human oral microbiome. Proceedings of the National Academy of Sciences 111, E2875–E2884. https://doi.org/10.1073/pnas.1409644111

Esberg, A., Barone, A., Eriksson, L., Holgerson, P.L., Teneberg, S., Johansson, I., 2020. Corynebacterium matruchotii demography and adhesion determinants in the oral cavity of healthy individuals. Microorganisms 8, 1–17. https://doi.org/10.3390/microorganisms8111780

Foster, J.S., Kolenbrander, P.E., 2004. Development of a multispecies oral bacterial community in a saliva-conditioned flow cell. Applied and Environmental Microbiology 70, 4340–4348. https://doi.org/10.1128/AEM.70.7.4340-4348.2004

Gibson, D.G., Young, L., Chuang, R.Y., Venter, J.C., Hutchison, C.A., Smith, H.O., 2009. Enzymatic assembly of DNA molecules up to several hundred kilobases. Nature Methods 6, 343–345. https://doi.org/10.1038/nmeth.1318

Guggenheim, B., Giertsen, E., Schüpbach, P., Shapiro, S., 2001. Validation of an in vitro biofilm model of supragingival plaque. Journal of Dental Research 80, 363–370. https://doi.org/10.1177/00220345010800011201

Iwami, Y., Higuchi, M., Yamada, T., Araya, S., 1972. Degradation of Lactate by Bacterionema matruchotii Under Aerobic and Anaerobic Conditions. Journal of Dental Research 51, 1683. https://doi.org/10.1177/00220345720510063901

Jakubovics, N.S., Gill, S.R., Vickerman, M.M., Kolenbrander, P.E., 2008. Role of hydrogen peroxide in competition and cooperation between Streptococcus gordonii and Actinomyces naeslundii. FEMS Microbiology Ecology 66, 637–644. https://doi.org/10.1111/j.1574-6941.2008.00585.x

Jett, B.D., Hatter, K.L., Huycke, M.M., Gilmore, M.S., 1997. Simplified agar plate method for quantifying viable bacteria. BioTechniques 23, 648–650.

569 Kim, D., Barraza, J.P., Arthur, R.A., Hara, A., Lewis, K., Liu, Y., Scisci, E.L., Hajishengallis, E.,
570 Whiteley, M., Koo, H., 2020. Spatial mapping of polymicrobial communities reveals a
571 precise biogeography associated with human dental caries. Proceedings of the National
572 Academy of Sciences of the United States of America 117.
573 https://doi.org/10.1073/pnas.1919099117
574 Kim, J., Connell, J.L., Whiteley, M., Bard, A.J., 2014. Development of a Versatile in Vitro Plat-
575 form for Studying Biological Systems Using Micro-3D Printing and Scanning Electro-
576 chemical Microscopy. Anal. Chem. 86, 12327–12333. https://doi.org/10.1021/ac5036204
577 Kim, J., Renault, C., Nioradze, N., Arroyo-Currás, N., Leonard, K.C., Bard, A.J., 2016. Nanome
578 ter scale scanning electrochemical microscopy instrumentation. Anal. Chem. 88, 10284-
579 10289. https://doi.org/10.1021/acs.analchem.6b03024
580 Kolenbrander, P.E., Palmer, R.J., Rickard, A.H., Jakubovics, N.S., Chalmers, N.I., Diaz, P.I.,
581 2006. Bacterial interactions and successions during plaque development. Periodontol-
582 ogy 2000 42, 47–79. https://doi.org/10.1111/j.1600-0757.2006.00187.x
583 Langmead, B., Salzberg, S.L., 2012. Fast gapped-read alignment with Bowtie 2. Nature Meth-
584 ods 9, 357–359. https://doi.org/10.1038/nmeth.1923
585 Love, M.I., Huber, W., Anders, S., 2014. Moderated estimation of fold change and dispersion for
586 RNA-seq data with DESeq2. Genome Biology 15, 1–21. https://doi.org/10.1186/s13059-
587 014-0550-8
588 Mark Welch, J.L., Rossetti, B.J., Rieken, C.W., Dewhirst, F.E., Borisy, G.G., 2016. Biogeogra-
589 phy of a human oral microbiome at the micron scale. Proceedings of the National Acad-
590 emy of Sciences of the United States of America 113, E791-800.
591 https://doi.org/10.1073/pnas.1522149113
592 Merritt, J.H., Kadouri, D.E., O'Toole, G.A., 2005. Growing and Analyzing Static Biofilms Judith.
593 Curr Protoc Microbiol 1–29. https://doi.org/10.1002/9780471729259.mc01b01s00.Grow-
594 ing
595 Morillo-lopez, V., Sjaarda, A., Borisy, G.G., Welch, J.M., 2021. Corncob structures in dental
596 plaque reveal microhabitat taxon specificity 1–23.
597 Puri, S.R., Kim, J., 2019. Kinetics of Antimicrobial Drug Ion Transfer at a Water/Oil Interface
598 Studied by Nanopipet Voltammetry. Anal. Chem. 91, 1873–1879.
599 https://doi.org/10.1021/acs.analchem.8b03593
600 Ramsey, M.M., Rumbaugh, K.P., Whiteley, M., 2011. Metabolite cross-feeding enhances viru-
601 lence in a model polymicrobial infection. PLoS Pathogens 7, 1–8.
602 https://doi.org/10.1371/journal.ppat.1002012
603 Redanz, S., Cheng, X., Giacaman, R.A., Pfeifer, C.S., Merritt, J., Kreth, J., 2018. Live and let
604 die: hydrogen peroxide production by the commensal flora and its role in maintaining a
605 symbiotic microbiome. Methods Molecular Biology 33, 337–352.
606 https://doi.org/10.1111/omi.12231.Live
607 Regev-Yochay, G., Trzcinski, K., Thompson, C.M., Lipsitch, M., Malley, R., 2007. SpxB is a sui-
608 cide gene of Streptococcus pneumoniae and confers a selective advantage in an in vivo
609 competitive colonization model. Journal of Bacteriology 189, 6532–6539.
610 https://doi.org/10.1128/JB.00813-07
611 Schgfer, A., Tauch, A., Jsger, W., Kalinowski, J., Thierbachb, G., Piihler, A., 1994. Small mobi-
612 lizable multi-purpose cloning vectors derived from the Escherichia coli plasmids pK18
613 and pK19: selection of defined deletions in the chromosome of Corynebacterium glu-
614 tumicum 145, 69–73.
615 Schoilew, K., Ueffing, H., Dalpke, A., Wolff, B., Frese, C., Wolff, D., Boutin, S., 2019. Bacterial
616 biofilm composition in healthy subjects with and without caries experience. Journal of
617 Oral Microbiology 11. https://doi.org/10.1080/20002297.2019.1633194
618 Shishkin, A.A., Giannoukos, G., Kucukural, A., Ciulla, D., Busby, M., Surka, C., Chen, J.,
619 Bhattacharyya, R.P., Rudy, R.F., Patel, M.M., Novod, N., Hung, D.T., Gnirke, A., Garber,

620 M., Guttman, M., Livny, J., 2015. Simultaneous generation of many RNA-seq libraries in
621 a single reaction. Nature Methods 12, 323–325. https://doi.org/10.1038/nmeth.3313
622 Smith, J.L., 2004. The physiological role of ferritin-like compounds in bacteria. Critical Reviews
623 in Microbiology 30, 173–185. https://doi.org/10.1080/10408410490435151
624 Takahashi, N., 2005. Microbial ecosystem in the oral cavity: Metabolic diversity in an ecological
625 niche and its relationship with oral diseases. International Congress Series 1284, 103–
626 112. https://doi.org/10.1016/j.ics.2005.06.071
627 Takayama, K., Hayes, B., Vestling, M.M., Massey, R.J., 2003. Transposon-5 mutagenesis
628 transforms Corynebacterium matruchotii to synthesize novel hybrid fatty acids that func-
629 tionally replace corynomycolic acid. The Biochemical journal 373, 465–474.
630 https://doi.org/10.1042/BJ20030248
631 Van Houte, J., Sansone, C., Joshipura, K., Kent, R., 1991. In vitro Acidogenic Potential and Mu-
632 tans Streptococci of Human Smooth-surface Plaque Associated with Initial Caries Le-
633 sions and Sound Enamel. Journal of Dental Research 70, 1497–1502.
634 https://doi.org/10.1177/00220345910700120501
635 Winterbourn, C.C., 1995. Toxicity of iron and hydrogen peroxide: the Fenton reaction. Toxicol-
636 ogy Letters 82–83, 969–974. https://doi.org/10.1016/0378-4274(95)03532-X
637 Xiao, C., Ran, S., Huang, Z., Liang, J., 2016. Bacterial diversity and community structure of su-
638 pragingival plaques in adults with dental health or caries revealed by 16S pyrosequenc-
639 ing. Frontiers in Microbiology 7, 1–15. https://doi.org/10.3389/fmicb.2016.01145
640 Zheng, Z., Stewart, P.S., 2002. Penetration of rifampin through Staphylococcus epidermidis bio-
641 films. Antimicrobial Agents and Chemotherapy 46, 900–903.
642 https://doi.org/10.1128/AAC.46.3.900-903.2002
643 Zhu, L., Kreth, J., 2012. The role of hydrogen peroxide in environmental adaptation of oral mi-
644 crobial communities. Oxidative Medicine and Cellular Longevity 2012.
645 https://doi.org/10.1155/2012/717843
646
647